Na^+-Cl^- cotransporter-mediated chloride uptake contributes to hypertension and renal damage in aldosterone-infused rats

Takahiro Yamauchi[1], Shigehiro Doi[1*], Ayumu Nakashima[1], Toshiki Doi[1], Eisei Sohara[2], Shinichi Uchida[2], Takao Masaki[1]

[1] Department of Nephrology, Hiroshima University Hospital, Hiroshima, Japan

[2] Department of Nephrology, Graduate School of Medical and Dental Sciences, Tokyo Medical and Dental University, Tokyo, Japan

Running head: Chloride and aldosterone nephropathy

*** Corresponding author**

Shigehiro Doi MD, PhD

Department of Nephrology, Hiroshima University Hospital

Address: 1-2-3 Kasumi Minami-ward, Hiroshima 734-8551, Japan

Telephone number: +81 82 257 1506 Fax number: +81 82 257 1508

E-mail address: sdoi@hiroshima-u.ac.jp

Authors' contributions

Conceived and designed the experiments: SD and TM. Performed the experiments: TY and TD. Analyzed the data: AN. Contributed reagents/materials/analysis tools: SU, ES, and SD. Wrote the paper: TY, SD, and TM.

Abstract

Recently, in addition to epithelial sodium channel alpha-subunit (αENaC), the thiazide-sensitive sodium-chloride cotransporter (NCC) and pendrin, also known as sodium-independent chloride/iodide transporter, were reported to be activated by aldosterone. Here, we investigated whether chloride (Cl^-) is responsible for hypertension, inflammation, and renal damage in aldosterone-infused rats. Following left nephrectomy, 8-week-old male Sprague-Dawley rats were allocated into four groups: 1) drinking 1.0% sodium chloride solution with aldosterone infusion (Aldo/NaCl rats); 2) drinking 1.44% sodium bicarbonate solution with aldosterone infusion (Aldo/$NaHCO_3$ rats); 3) drinking distilled water with aldosterone infusion (Aldo/water rats); and 4) drinking distilled water without aldosterone infusion (sham rats). Additionally, hemi-nephrectomized rats with aldosterone infusion were fed a 0.26% NaCl diet (control); 8.0% NaCl diet (high-Na/high-Cl); or a 4.0% NaCl 6.67% sodium citrate diet (high-Na/half-Cl). Last, Aldo/NaCl rats were treated with or without hydrochlorothiazide. Blood pressure in the Aldo/NaCl rats was significantly higher than in the Aldo/$NaHCO_3$ rats, which was associated with the increased expression of NCC. Expression of markers of inflammation (CD3, CD68, interleukin-17A) and fibrosis (α-smooth muscle actin, collagen 1) were also increased in Aldo/NaCl rats. Similarly, aldosterone-infused rats fed a high-Na/half-Cl diet had lower blood pressure than those fed a high-Na/high-Cl diet, with a reduction of phosphorylated-NCC, but not αENaC and pendrin. NCC inhibition with hydrochlorothiazide attenuated interleukin-17A protein expression along with the phosphorylation of NCC in Aldo/NaCl rats. These findings suggest that NCC-mediated Cl^- uptake plays important roles in the development of aldosterone-induced hypertension and renal injury.

Keywords: chloride; sodium-chloride cotransporter; aldosterone; hypertension; inflammation

Introduction

The kidneys retain the balance between salt and water within body fluid, playing an important role in maintaining blood pressure. Excessive dietary salt intake is a well-known major factor for the induction of hypertension. Guyton et al. first proposed that a decrease in renal excretion of salt leads to fluid retention, resulting in hypertension through an increase in cardiac output (15). Several studies have demonstrated that salt susceptibility to hypertension, also called 'salt-sensitivity', is different in each person (8), and that salt-sensitive hypertension is caused by several factors, including activation of the sympathetic nervous system, the renin-angiotensin-aldosterone system, and hyperinsulinemia (3, 17, 28). However, the precise mechanisms behind salt-sensitivity remain unclear.

A recent study suggested that dietary salt *per se* accelerates sodium (Na^+) reabsorption through RAS-related C3 botulinum toxin substrate 1 activation in the salt-sensitive phenotype (31). Dietary salt comprises both Na^+ and chloride (Cl^-) ions, and their excretion is regulated at distal nephrons, which consists of a distal tubule and a collecting duct. Although Na^+ is considered to be a major contributor to hypertension, previous studies suggest that Cl^-, rather than Na^+, is essential for maintaining blood pressure and volume retention (6, 42). Studies also report that selective Cl^- loading causes vasocontraction and microangiopathy in spontaneously hypertensive rats (30, 35). In contrast, oral intake of sodium bicarbonate ($NaHCO_3$) did not elevate blood pressure in rats treated with deoxycorticosterone acetate (DOCA) (45). These findings raise the possibility that the dual roles of NaCl in the pathogenesis of salt-sensitive hypertension may be explained by Cl^- reabsorption at the distal nephron.

Among the various models of salt-sensitive hypertension, aldosterone/salt-treated animals exhibit infiltration of the kidneys by numerous immune cells, including lymphocytes and

macrophages (4). A previous study found that administration of mycophenolate mofetil (MMF), an immunosuppressant, ameliorated aldosterone/salt-induced hypertension (5). We also reported that another immunosuppressive agent, mizoribine, attenuated not only renal inflammation but also hypertension in a rat aldosterone/NaCl model (10). These findings suggest that aldosterone/NaCl-induced inflammation may be implicated in the development of hypertension (13). Notably, recent studies have demonstrated that excess intake of NaCl causes inflammation through upregulation of interleukin-17A (IL-17A) derived from Th17 cells (1, 23). However, the role of Cl^- on renal inflammation and hypertension in aldosterone-infused rats remains unclear.

In this study, we investigated whether Cl^- is responsible for the observed hypertension, inflammation, and renal damage in aldosterone-infused rats. We found that administration of $NaHCO_3$ solution resulted in less renal inflammation, fibrosis, and hypertension in aldosterone-infused rats compared with administration of NaCl. Next, we show that a 4.0% NaCl 6.67% sodium citrate (high-Na/half-Cl) diet had less hypertension compared with an 8.0% NaCl (high-Na/high-Cl) diet in aldosterone-infused rats. Last, Na^+-Cl^- cotransporter (NCC) inhibition with hydrochlorothiazide (HCTZ) attenuated IL-17A protein expression in aldosterone/NaCl-infused rats. Both Cl^- restriction and HCTZ administration attenuated protein expression of functional phosphorylated NCC in the membrane fraction. These results suggest that NCC-mediated Cl^- uptake plays important roles in the development of aldosterone-induced hypertension and renal injury.

Materials and methods

Ethical considerations

All experiments were carried out in accordance with recommendations for the Care and Use of

95 Laboratory Animals in the National Institutes of Health Guidelines. The Institutional Animal
96 Care and Use Committee of Hiroshima University (Hiroshima, Japan) approved the experimental
97 protocols (Permit Number: A10-52). All efforts were taken to minimize pain and distress to
98 animals.
99
100 ***Surgical procedures***
101 Eight-week-old male Sprague-Dawley rats (290–320 g) were purchased from Charles River
102 Laboratories Japan (Yokohama, Japan). Rats underwent left nephrectomy under anesthesia with
103 an intraperitoneal injection of sodium pentobarbital or a medetomidine-midazolam-butorphanol
104 combination. Aldosterone (Sigma-Aldrich, St. Louis, MO) was dissolved in distilled water
105 containing dimethyl sulfoxide, and the solution was administered to rats using ALZET™
106 osmotic pumps (Durect, Cupertino, CA) (10). Pumps were subcutaneously implanted in rats,
107 ensuring constant aldosterone infusion throughout the six-week study period.
108
109 ***Experimental protocol***
110 *Experiment 1*: Following surgery, rats were allocated into four groups: 1) drinking 1.0% NaCl
111 solution with aldosterone infusion (Aldo/NaCl rats, n = 8); 2) drinking 1.44% $NaHCO_3$ solution
112 with aldosterone infusion (Aldo/$NaHCO_3$ rats, n = 8); 3) drinking distilled water with
113 aldosterone infusion (Aldo/water rats, n = 7); and 4) drinking distilled water without aldosterone
114 infusion (sham rats, n = 8). The concentration of Na^+ in solutions was adjusted to match
115 equimolecular amounts between Aldo/NaCl rats and Aldo/$NaHCO_3$ rats. The amount of NaCl in
116 the standard rat chow was 0.30% (Oriental Yeast Co., Ltd, Tokyo, Japan). At the end of the fifth
117 week, rats were killed by cardiac puncture under deep anesthesia.

Experiment 2: Aldosterone-infused, hemi-nephrectomized rats were divided into three groups: 1) 0.26% NaCl (0.10% Na/0.16% Cl) diet (control rats, n = 8); 2) 8.0% NaCl (3.14% Na/4.85% Cl) diet (high-Na/high-Cl rats, n = 8); and 3) 4.0% NaCl 6.67% sodium citrate (3.14% Na/2.43% Cl) diet (high-Na/half-Cl rats, n = 8) **(Table 1)**. The formula diets were provided by Research Diets, Inc. (New Brunswick, NJ). At the end of the sixth week, rats were killed by cardiac puncture under deep anesthesia.

Experiment 3: We inhibited NCC by administering HCTZ (Sigma-Aldrich). Aldo/NaCl rats were generated as above. At two weeks into the study, Aldo/NaCl rats were divided into two groups. Distilled water (vehicle-treated rats, n = 4) or 25 mg/kg/day HCTZ in distilled water (HCTZ-treated rats, n = 5) was administrated by oral gavage. At the end of the fifth week, rats were killed by cardiac puncture under deep anesthesia.

Measurement of biological parameters

Blood pressure was measured weekly (*Experiment 1* and *3*) or biweekly (*Experiment 2*) using the tail cuff method (Softron, Tokyo, Japan). Twenty-four-hour urine samples were collected using metabolic cages (Natsume, Tokyo, Japan). Rats were kept in the metabolic cages for one day of acclimatization prior to starting urine collection. At the end of the fifth (*Experiment 1* and *3*) or the sixth (*Experiment 2*) week, blood samples were taken by cardiac puncture. Measurement of blood and urine samples was outsourced to SRL Inc. (Tokyo, Japan). Blood pH was analyzed by I-STAT (chem 8+ cartridge; Abbott Point of Care, Princeton, NJ).

Histological examination

Renal tissue samples were processed to formalin-fixed, paraffin-embedded sections. Two-μm-

thick paraffin sections were prepared for light microscopy and stained with hematoxylin and eosin (H-E), Masson's trichrome (M-T), and periodic acid-Schiff (PAS). Twenty glomeruli under a high-power field (original magnification ×200) were selected from sections of rat kidneys. All microscopic images were captured using Lumina Vision 2.20 (Mitani, Fukui, Japan). Glomerular injury was evaluated using a glomerulosclerosis scoring system reported previously (24). Briefly, glomeruli stained with PAS were graded on a scale of 0 to 4: 0, normal; 1, involvement of 1%-25% of glomerular tufts; 2, involvement of 26%–50% of glomerular tufts; 3, involvement of 51%–75% of glomerular tufts; 4, involvement of 75%–100% of glomerular tufts. The scorer did not know the treatment group when scoring.

Immunohistochemistry

Paraffin sections (4 μm thick) were subjected to immunohistochemical staining as previously described (10, 38). Primary antibodies used were: mouse monoclonal anti-human CD3 antibody (1:5000; Dako, Glostrup, Denmark), mouse monoclonal anti-human CD68 antibody (1:2000; AbD Serotec, Oxford, UK), mouse monoclonal anti-alpha-smooth muscle actin (αSMA) antibody (1:10000; Sigma-Aldrich), and rabbit polyclonal anti-collagen 1 antibody (1:2000; Abcam, Cambridge, UK). CD3, CD68, and αSMA were detected using the Envision System (Dako). Collagen 1 was stained using the avidin-biotin complex method. To detect death cells in the kidney, terminal deoxynucleotidyl transferase dUTP nick-end labeling (TUNEL) staining was performed using the DeadEnd Colorimetric TUNEL System (Promega, Madison, WI), according to the manufacturer's instructions.

The CD3-, CD68-, and TUNEL-positive cells were counted in 10 selected fields of the cortex (×100) that were captured using a Lumina Vision 2.20 (Mitani). αSMA- and collagen 1-

positively stained areas were assessed in five selected fields of the cortex (×40) and those of the corticomedullary junction (×40), were also captured as above. Quantitative analysis was performed using Image J software (National Institutes of Health, Bethesda, MD).

Immunoblot assays

To extract protein from whole tissue, frozen renal tissue samples were lysed in cell lysis buffer (Cell Signaling Technology, Danvers, MA) and homogenized for 40 s using an ultrasonic homogenizer (VP-050; Taitec, Saitama, Japan) at 20% power. Soluble protein was additionally sonicated for 20 s. Protein from the membrane fraction was extracted using a Minute™ plasma membrane protein isolation kit (Invent Biotechnologies, Plymouth, MN). The concentration of the protein solution was measured using a Pierce™ BCA protein assay kit (Thermo Fisher Scientific, Rockford, IL), and then the concentration was adjusted uniformly. An equal amount of each sample was analyzed by immunoblot analysis, as previously described (10, 38).

The primary antibodies used were: rabbit polyclonal anti-epithelial sodium channel-α antibody (1:2500; StressMarq Biosciences, Victoria, BC, Canada); rabbit polyclonal anti-slc26A4 antibody (1:4000; Bioss, Woburn, MA); rabbit polyclonal anti-thiazide-sensitive Na^+-Cl^- cotransporter antibody (1:2000; EMD Millipore, Darmstadt, Germany); mouse monoclonal anti-αSMA antibody (1:5000; Sigma-Aldrich); and mouse monoclonal anti-IL-17A antibody (1:2000; Novus Biologicals, Littleton, CO). Mouse polyclonal anti-alpha-glyceraldehyde-3-phosphate dehydrogenase (GAPDH) antibody (1:10000; Sigma-Aldrich) was used as a reference standard for protein derived from whole renal lysate. Rabbit polyclonal anti-phosphorylated-NCC antibodies, specifically anti-Thr53-NCC (1:2000), anti-Thr58-NCC (1:1000), and anti-Per71-NCC (1:2000) were as described previously (7). The secondary antibodies were biotin-

conjugated goat anti-rabbit immunoglobulin G (H+L) antibody (Thermo Fisher Scientific) and HRP-conjugated goat anti-mouse immunoglobulin G (H+L) antibody (Thermo Fisher Scientific). Signals were detected using the SuperSignal West Dura and Pico system (Thermo Fisher Scientific). The intensity of each protein band was measured using Image J software (National Institutes of Health).

Statistical analysis

Results for parametric data are expressed as the means ± standard deviation (SD) for each group of rats. Statistical analysis was performed using SPSS (version 22.0; IBM, Armonk, NY). Comparisons between two groups were tested using Student's *t*-test, while those among groups were tested by analysis of variance (ANOVA) followed by Tukey's post hoc test. The glomerulosclerosis score was analyzed by Kruskal-Wallis analysis followed by the Steel-Dwass test. The general linear model was applied for comparisons of blood pressure values and urinary samples at each time point and each group. Values of $P < 0.05$ were considered to be statistically significant.

Results

NaCl, but not $NaHCO_3$, induced hypertension in aldosterone-infused rats

We first evaluated the effect of NaCl and $NaHCO_3$ on the physical characteristics of aldosterone-infused rats. At the fifth week, Aldo/NaCl rats demonstrated lower body weights compared with Aldo/$NaHCO_3$ rats. Moreover, severe renal hypertrophy was observed in Aldo/NaCl rats. Although the serum Na^+ concentration did not show any significant differences among the groups, serum levels of potassium (K^+) and Cl^- were lower in Aldo/NaCl and Aldo/$NaHCO_3$ rats

than in sham and Aldo/water rats **(Table 2)**.

Systolic blood pressure values in Aldo/NaCl rats gradually rose during the observation period. From week 2, blood pressure values showed a significant increase in the Aldo/NaCl rats compared with the Aldo/$NaHCO_3$ rats **(Fig. 1A)**. The urinary excretion of Na^+ and Cl^- was increased in Aldo/NaCl rats, however K^+ did not differ. Urinary protein excretion was also significantly increased in Aldo/NaCl rats **(Fig. 1B)**.

Expression of NCC and αENaC, but not pendrin, was increased in Aldo/NaCl rats compared with Aldo/$NaHCO_3$ rats

Although aldosterone is known to upregulate the expression of NCC, αENaC, and pendrin, the effect of $NaHCO_3$ on expression of these factors in aldosterone-infused rats remains unclear. We extracted proteins located in the membrane fraction from renal samples and adjusted the protein concentration of each sample. Expression levels of transporter proteins from the membrane lysates were examined using immunoblot analysis. Total-NCC expression in membrane lysates was significantly increased in Aldo/NaCl rats compared with Aldo/$NaHCO_3$ rats, while αENaC and pendrin expression did not differ significantly between the two groups **(Fig. 2A** and **B)**. To evaluate the activated form of NCC, we examined expression levels of phosphorylated-NCC proteins, specifically T53-NCC, T58-NCC, and P71-NCC. The expression of phosphorylated-NCC proteins were higher in Aldo/NaCl rats than in Aldo/$NaHCO_3$ and Aldo/water rats **(Fig. 2C** and **D)**.

Number of Cell Death and expression of fibrotic markers were increased in the kidneys of Aldo/NaCl rats compared with Aldo/$NaHCO_3$ rats

To evaluate renal injury, formalin-fixed, paraffin-embedded tissues were processed for histological analysis. By H-E staining, Aldo/NaCl rats displayed an increase in renal tubular dilation and immune cell infiltration into the tubulointerstitium compared with Aldo/$NaHCO_3$ and Aldo/water rats **(Fig. 3A)**. Kidneys from Aldo/NaCl rats showed large areas stained with aniline blue after M-T staining, which indicated fibrotic tissue **(Fig. 3A)**. Some glomeruli from Aldo/NaCl rats demonstrated marked glomerulosclerosis and adhesions to the Bowman's capsule along with focal tubulointerstitial injury, such as tubular dilation and protein casts **(Fig. 3A)**. Conversely, Aldo/$NaHCO_3$ and Aldo/water rats showed few sclerotic changes **(Fig. 3B)**.

Immunohistochemical staining was performed to investigate renal injury more closely. TUNEL staining was performed to determine cell death. TUNEL-positive cells were observed mainly in the tubulointerstitium **(Fig. 3C)**. Kidneys from Aldo/NaCl rats had more TUNEL-positive cells than Aldo/$NaHCO_3$ rats **(Fig. 3D)**. To assess the effects of NaCl and $NaHCO_3$ on fibrosis in aldosterone-infused rats, the expression of αSMA and collagen 1 were used as markers of myofibroblasts and extracellular matrix protein, respectively. While increased areas of fibrosis were observed in the renal tubulointerstitium of Aldo/NaCl rats, there were few fibrotic changes in Aldo/$NaHCO_3$ rats **(Fig. 3C** and **D)**. Protein expression of αSMA was also examined by immunoblot assay and the findings were compatible with the results from immunohistochemical staining **(Fig. 3E** and **F)**.

Renal inflammation was increased in Aldo/NaCl rats compared with Aldo/$NaHCO_3$ rats

T cell-mediated inflammation and macrophage migration into the kidneys are dominant pathophysiological features in the development of salt-sensitive hypertension. It has recently been reported that differentiation of naïve T cells into T helper 17 (Th17) cells is central to

256 inflammation in the salt-sensitive state (18). Therefore, we performed immunohistochemical
257 staining for CD3, a maker of T lymphocytes, and CD68, a marker of macrophages and
258 monocytes. Aldo/NaCl rats demonstrated numerous CD3- and CD68-positive cells infiltrating
259 the tubulointerstitium of the kidneys **(Fig. 4A** and **B)**. Expression of IL-17A was also upregulated
260 in Aldo/NaCl rats, however IL-17A expression in the Aldo/$NaHCO_3$ rats did not differ from the
261 Aldo/water rats **(Fig. 4C** and **D)**.
262
263 ***Dietary Cl^- restriction suppressed hypertension and inhibited NCC phosphorylation in***
264 ***aldosterone-infused rats with Na^+ overload.***
265 To confirm the effect of Cl^- on salt-sensitive hypertension under conditions of equalized Na^+
266 overload, we measured blood pressure and examined the expression of NCC, αENaC, and
267 pendrin in rats on control, high-Na/high-Cl, and high-Na/half-Cl diets. During the observation
268 period, dietary consumption and body weight were not significantly different between the high-
269 Na/high-Cl and high-Na/half-Cl groups **(Fig. 5A** and **Table 3)**. At the third week, urinary
270 excretion of Na^+ did not differ between the high-Na/high-Cl and high-Na/half-Cl rats, whereas
271 urinary Cl^- was increased in high-Na/high-Cl rats compared with high-Na/half-Cl rats **(Table 3)**.
272 Similar to Aldo/NaCl rats, blood pressure of high-Na/high-Cl rats was higher than that of high-
273 Na/half-Cl rats **(Fig. 5B)**. By immunoblot analysis, phosphorylated-NCC expression in
274 membrane lysates were significantly upregulated in high-Na/high-Cl rats compared with high-
275 Na/half-Cl rats **(Fig. 5C** and **D)**.
276
277
278 ***HCTZ alleviated hypertension and attenuated αSMA and IL-17A expression***

279 To determine the role of NCC in Aldo/NaCl rats, we investigated the effect of HCTZ on blood
280 pressure and renal inflammation and damage. Oral administration of HCTZ, a pharmacological
281 inhibitor of NCC, at a dose of 25 mg/kg/day for four weeks suppressed the rise in blood pressure
282 in Aldo/NaCl rats, along with reduced urinary protein excretion **(Fig. 6A** and **B)**. Immunoblot
283 assays also revealed that, in addition to αSMA, IL-17A decreased in HCTZ-treated rats
284 compared with vehicle-treated rats **(Fig. 6C)**.
285
286 ***HCTZ suppressed phosphorylated-NCC expression in the membrane fraction***
287 To identify the inhibitory effect of NCC on transporters at the distal nephron in Aldo/NaCl rats,
288 we investigated the protein expression of NCC, αENaC, and pendrin between vehicle-treated and
289 HCTZ-treated rats. Although expression levels of total- and phosphorylated-NCC in membrane
290 lysates were significantly decreased in HCTZ-treated rats, those of αENaC and pendrin did not
291 change, irrespective of HCTZ treatment **(Fig. 7A** and **B)**.
292
293 **Discussion**
294 In this study, we found that aldosterone-induced salt-sensitive hypertension increased in rats
295 administered NaCl, but not $NaHCO_3$, in their drinking water which was accompanied by
296 significantly increased expression of NCC. Administration of NaCl, but not $NaHCO_3$, increased
297 not only renal fibrosis but also infiltration of inflammatory cells along with upregulated
298 expression of IL-17A in aldosterone-infused rats. Similarly, even with the equimolar Na^+
299 overloading, a high-Na/high-Cl diet showed higher blood pressure than the high-Na/half-Cl diet
300 in aldosterone-infused rats. High-Na/high-Cl diet upregulated expression of phosphorylated
301 NCC, whereas the high-Na/half-Cl diet did not. Last, NCC inhibition with HCTZ improved

hypertension, renal fibrosis, and inflammation in Aldo/NaCl rats. These findings suggest that NCC-mediated Cl^- reabsorption plays a pivotal role in the development of hypertension and renal damage in this rat model of aldosterone-induced salt-sensitive hypertension.

We found that Aldo/NaCl treatment induced elevated blood pressure and increased the expression of NCC and pendrin compared with Aldo/water treatment. Among several inducers of salt-sensitive hypertension, aldosterone is well-known to increase renal NaCl reabsorption through activating αENaC and NCC (7, 9, 20). Thus, exogenous aldosterone infusion is regularly used for animal models of salt-sensitive hypertension. Recently, DOCA was reported to increase expression levels of pendrin in mice (27, 41). Previous studies have demonstrated that pendrin enhances γENaC function, possibly through its ability to keep channels open and alter subcellular protein distribution (25), and that elevated blood pressure is not observed in pendrin-null mice with DOCA/NaCl treatment (41). In contrast, other studies have reported that specific deletion of the pendrin gene did not attenuate salt-sensitive hypertension (32, 44). Therefore, the role of pendrin on the progression of hypertension remains controversial. In the current study, we found that in rats that drank $NaHCO_3$, or had the high-Na/half-Cl diet or received HCTZ treatment, salt-sensitive hypertension improved without changes in pendrin expression. Taken together, the results suggest that pendrin is not likely to be responsible for Aldo/NaCl-induced hypertension.

Aldo/$NaHCO_3$ and high-Na/half-Cl rats did not show significant elevations in blood pressure nor did they show upregulation of NCC, indicating that, in addition to aldosterone, Cl^- is essential for increased salt-sensitivity through activation of NCC. We also observed that inhibition of NCC with oral administration of HCTZ attenuated not only hypertension and renal damage, including proteinuria, interstitial fibrosis and inflammation, in Aldo/NaCl rats but also

reduced total- and phosphorylated-NCC expression. NCC phosphorylation is induced by various stimuli, including hypokalemia, aldosterone, angiotensin, hyperinsulinemia, and sympathetic stimulation, which are all known to contribute to salt sensitivity (22, 34, 36, 37, 39). Our data indicate that NCC-mediated Cl^- reabsorption plays an important role in the development of salt-sensitive hypertension.

Previous research has shown that NCC knockout mice upregulate not only γENaC expression but also pendrin expression (14). Additionally, aldosterone-induced alkalosis leads to enhanced expression of pendrin (29, 41). These findings suggest that either γENaC or pendrin are complementarily overexpressed to retain NaCl as well as to maintain acid-base homeostasis during blocking of the NCC function (32). However, in the current study, NCC inhibition with HCTZ was not compensated for by increased expression of γENaC (data not shown) and pendrin. One possible explanation for this finding is that the biological half-life of oral HCTZ is only 1.7 and 13.1 hours for the α- and β-phases, respectively, indicating that HCTZ administration only has a temporary inhibitory effect on NCC, unlike that observed in knockout animals (2). Another possible mechanism is that γENaC and pendrin might have already been upregulated in Aldo/NaCl rats. In either case, our data suggest that γENaC and pendrin do not confer the ability to compensate for NCC.

Previous studies found that administration of DOCA or angiotensin II could not induce hypertension in rodents lacking T and B lymphocytes (16, 33). It is also reported that immunosuppressants, such as TNF-α inhibitors, MMF or mizoribine, prevent hypertension in salt-sensitive animal models (5, 10, 11). Importantly, recent studies have clarified that NaCl promotes autoimmune disease through Th17 (18), and that deletion of IL-17A ameliorates hypertension and renal injury in DOCA/NaCl rats (1). These findings suggest that T cell-driven

inflammation is involved in aldosterone-induced hypertension. In the current study, the protein expression level of IL-17A was suppressed in Aldo/$NaHCO_3$ rats and Aldo/NaCl rats with HCTZ treatment. Taken together, it appears that Cl^- plays an essential role in the development of salt-induced inflammation.

Dysregulated Th17 cells are regarded as a therapeutic target not only for salt-sensitive hypertension but also inflammatory renal diseases, including lupus nephritis, IgA nephropathy, crescentic glomerulonephritis, and post-transplant rejection (12, 19, 26, 40). Chronic inflammation is recognized to cause subsequent fibrosis through production of transforming growth factor-β1 (21). A recent study reported that T cells are required for both collagen deposition and hypertension (43). Anti-inflammatory therapies suppress renal fibrosis, suggesting that inhibition of T cells, at least in part, has anti-fibrotic effects. These findings raise the possibility that Cl^--mediated inflammation contributes to renal fibrosis as well as salt-sensitive hypertension.

In conclusion, aldosterone-infused rats with NaCl in their drinking water had increased hypertension and renal inflammation compared with $NaHCO_3$-treated controls. Reduction of dietary Cl^- also decreased the development of hypertension as well as NCC activation, even with equimolar Na^+ overloading. As activation of T lymphocytes is known to participate in the development of both hypertension and renal damage, Cl^- overload may also be involved in this critical process. HCTZ treatment was found to ameliorate blood pressure elevation and renal damage through the reduction of NCC expression. These results suggest that NCC-mediated Cl^- reabsorption plays an important role in the pathogenesis of salt-sensitive hypertension.

Acknowledgments

None.

Grants

This work was supported by the Tsuchiya Memorial Medical Foundation.

Disclosures

The authors declare no actual or potential conflicts of interest.

References

1. **Amador CA, Barrientos V, Pena J, Herrada AA, Gonzalez M, Valdes S, Carrasco L, Alzamora R, Figueroa F, Kalergis AM, and Michea L**. Spironolactone decreases DOCA-salt-induced organ damage by blocking the activation of T helper 17 and the downregulation of regulatory T lymphocytes. *Hypertension* 63: 797-803, 2014.

2. **Beermann B, Groschinsky-Grind M, and Rosen A**. Absorption, metabolism, and excretion of hydrochlorothiazide. *Clin Pharmacol Ther* 19: 531-537, 1976.

3. **Bigazzi R, Bianchi S, Baldari G, and Campese VM**. Clustering of cardiovascular risk factors in salt-sensitive patients with essential hypertension: role of insulin. *Am J Hypertens* 9: 24-32, 1996.

4. **Blasi ER, Rocha R, Rudolph AE, Blomme EA, Polly ML, and McMahon EG**. Aldosterone/salt induces renal inflammation and fibrosis in hypertensive rats. *Kidney Int* 63: 1791-1800, 2003.

5. **Boesen EI, Williams DL, Pollock JS, and Pollock DM**. Immunosuppression with mycophenolate mofetil attenuates the development of hypertension and albuminuria in

394 deoxycorticosterone acetate-salt hypertensive rats. *Clin Exp Pharmacol Physiol* 37: 1016-1022,
395 2010.
396 6. **Bruner CA, Weaver JM, and Fink GD**. Sodium-dependent hypertension produced by
397 chronic central angiotensin II infusion. *Am J Physiol* 249: H321-327, 1985.
398 7. **Chiga M, Rai T, Yang SS, Ohta A, Takizawa T, Sasaki S, and Uchida S**. Dietary salt
399 regulates the phosphorylation of OSR1/SPAK kinases and the sodium chloride cotransporter
400 through aldosterone. *Kidney Int* 74: 1403-1409, 2008.
401 8. **Chrysant SG, Walsh GM, Kem DC, and Frohlich ED**. Hemodynamic and metabolic
402 evidence of salt sensitivity in spontaneously hypertensive rats. *Kidney Int* 15: 33-37, 1979.
403 9. **Diakov A, and Korbmacher C**. A novel pathway of epithelial sodium channel
404 activation involves a serum- and glucocorticoid-inducible kinase consensus motif in the C
405 terminus of the channel's alpha-subunit. *J Biol Chem* 279: 38134-38142, 2004.
406 10. **Doi T, Doi S, Nakashima A, Ueno T, Yokoyama Y, Kohno N, and Masaki T**.
407 Mizoribine ameliorates renal injury and hypertension along with the attenuation of renal caspase-
408 1 expression in aldosterone-salt-treated rats. *PLoS One* 9: e93513, 2014.
409 11. **Elmarakby AA, Quigley JE, Imig JD, Pollock JS, and Pollock DM**. TNF-alpha
410 inhibition reduces renal injury in DOCA-salt hypertensive rats. *Am J Physiol Regul Integr Comp*
411 *Physiol* 294: R76-83, 2008.
412 12. **Espinosa A, Dardalhon V, Brauner S, Ambrosi A, Higgs R, Quintana FJ, Sjostrand**
413 **M, Eloranta ML, Ni Gabhann J, Winqvist O, Sundelin B, Jefferies CA, Rozell B, Kuchroo**
414 **VK, and Wahren-Herlenius M**. Loss of the lupus autoantigen Ro52/Trim21 induces tissue
415 inflammation and systemic autoimmunity by disregulating the IL-23-Th17 pathway. *J Exp Med*
416 206: 1661-1671, 2009.

13. **Franco M, Tapia E, Bautista R, Pacheco U, Santamaria J, Quiroz Y, Johnson RJ, and Rodriguez-Iturbe B**. Impaired pressure natriuresis resulting in salt-sensitive hypertension is caused by tubulointerstitial immune cell infiltration in the kidney. *Am J Physiol Renal Physiol* 304: F982-990, 2013.

14. **Grimm PR, Lazo-Fernandez Y, Delpire E, Wall SM, Dorsey SG, Weinman EJ, Coleman R, Wade JB, and Welling PA**. Integrated compensatory network is activated in the absence of NCC phosphorylation. *J Clin Invest* 125: 2136-2150, 2015.

15. **Guyton AC, Cowley AW, Jr., Coleman TG, DeClue JW, Norman RA, and Manning RD**. Hypertension: a disease of abnormal circulatory control. *Chest* 65: 328-338, 1974.

16. **Guzik TJ, Hoch NE, Brown KA, McCann LA, Rahman A, Dikalov S, Goronzy J, Weyand C, and Harrison DG**. Role of the T cell in the genesis of angiotensin II induced hypertension and vascular dysfunction. *J Exp Med* 204: 2449-2460, 2007.

17. **Imanishi M, Okada N, Konishi Y, Morikawa T, Maeda I, Kitabayashi C, Masada M, Shirahashi N, Wilcox CS, and Nishiyama A**. Angiotensin II receptor blockade reduces salt sensitivity of blood pressure through restoration of renal nitric oxide synthesis in patients with diabetic nephropathy. *J Renin Angiotensin Aldosterone Syst* 14: 67-73, 2013.

18. **Kleinewietfeld M, Manzel A, Titze J, Kvakan H, Yosef N, Linker RA, Muller DN, and Hafler DA**. Sodium chloride drives autoimmune disease by the induction of pathogenic TH17 cells. *Nature* 496: 518-522, 2013.

19. **Lin FJ, Jiang GR, Shan JP, Zhu C, Zou J, and Wu XR**. Imbalance of regulatory T cells to Th17 cells in IgA nephropathy. *Scand J Clin Lab Invest* 72: 221-229, 2012.

20. **Masilamani S, Kim GH, Mitchell C, Wade JB, and Knepper MA**. Aldosterone-mediated regulation of ENaC alpha, beta, and gamma subunit proteins in rat kidney. *J Clin Invest*

104: R19-23, 1999.

21. **Meng XM, Huang XR, Xiao J, Chung AC, Qin W, Chen HY, and Lan HY**. Disruption of Smad4 impairs TGF-beta/Smad3 and Smad7 transcriptional regulation during renal inflammation and fibrosis in vivo and in vitro. *Kidney Int* 81: 266-279, 2012.

22. **Nishida H, Sohara E, Nomura N, Chiga M, Alessi DR, Rai T, Sasaki S, and Uchida S**. Phosphatidylinositol 3-kinase/Akt signaling pathway activates the WNK-OSR1/SPAK-NCC phosphorylation cascade in hyperinsulinemic db/db mice. *Hypertension* 60: 981-990, 2012.

23. **Norlander AE, Saleh MA, Kamat NV, Ko B, Gnecco J, Zhu L, Dale BL, Iwakura Y, Hoover RS, McDonough AA, and Madhur MS**. Interleukin-17A Regulates Renal Sodium Transporters and Renal Injury in Angiotensin II-Induced Hypertension. *Hypertension* 68: 167-174, 2016.

24. **Ophascharoensuk V, Pippin JW, Gordon KL, Shankland SJ, Couser WG, and Johnson RJ**. Role of intrinsic renal cells versus infiltrating cells in glomerular crescent formation. *Kidney Int* 54: 416-425, 1998.

25. **Pech V, Wall SM, Nanami M, Bao HF, Kim YH, Lazo-Fernandez Y, Yue Q, Pham TD, Eaton DC, and Verlander JW**. Pendrin gene ablation alters ENaC subcellular distribution and open probability. *Am J Physiol Renal Physiol* 309: F154-163, 2015.

26. **Pekalski M, Jenkinson SE, Willet JD, Poyner EF, Alhamidi AH, Robertson H, Ali S, and Kirby JA**. Renal allograft rejection: examination of delayed differentiation of Treg and Th17 effector T cells. *Immunobiology* 218: 303-310, 2013.

27. **Pelzl L, Pakladok T, Pathare G, Fakhri H, Michael D, Wagner CA, Paulmichl M, and Lang F**. DOCA sensitive pendrin expression in kidney, heart, lung and thyroid tissues. *Cell Physiol Biochem* 30: 1491-1501, 2012.

28. **Piccirillo G, Bucca C, Durante M, Santagada E, Munizzi MR, Cacciafesta M, and Marigliano V**. Heart rate and blood pressure variabilities in salt-sensitive hypertension. *Hypertension* 28: 944-952, 1996.

29. **Procino G, Milano S, Tamma G, Dossena S, Barbieri C, Nicoletti MC, Ranieri M, Di Mise A, Nofziger C, Svelto M, Paulmichl M, and Valenti G**. Co-regulated pendrin and aquaporin 5 expression and trafficking in Type-B intercalated cells under potassium depletion. *Cell Physiol Biochem* 32: 184-199, 2013.

30. **Schmidlin O, Tanaka M, Bollen AW, Yi SL, and Morris RC, Jr.** Chloride-dominant salt sensitivity in the stroke-prone spontaneously hypertensive rat. *Hypertension* 45: 867-873, 2005.

31. **Shibata S, Mu S, Kawarazaki H, Muraoka K, Ishizawa K, Yoshida S, Kawarazaki W, Takeuchi M, Ayuzawa N, Miyoshi J, Takai Y, Ishikawa A, Shimosawa T, Ando K, Nagase M, and Fujita T**. Rac1 GTPase in rodent kidneys is essential for salt-sensitive hypertension via a mineralocorticoid receptor-dependent pathway. *J Clin Invest* 121: 3233-3243, 2011.

32. **Soleimani M, Barone S, Xu J, Shull GE, Siddiqui F, Zahedi K, and Amlal H**. Double knockout of pendrin and Na-Cl cotransporter (NCC) causes severe salt wasting, volume depletion, and renal failure. *Proc Natl Acad Sci U S A* 109: 13368-13373, 2012.

33. **Svendsen UG**. Evidence for an initial, thymus independent and a chronic, thymus dependent phase of DOCA and salt hypertension in mice. *Acta Pathol Microbiol Scand A* 84: 523-528, 1976.

34. **Talati G, Ohta A, Rai T, Sohara E, Naito S, Vandewalle A, Sasaki S, and Uchida S**. Effect of angiotensin II on the WNK-OSR1/SPAK-NCC phosphorylation cascade in cultured

mpkDCT cells and in vivo mouse kidney. *Biochem Biophys Res Commun* 393: 844-848, 2010.

35. **Tanaka M, Schmidlin O, Olson JL, Yi SL, and Morris RC**. Chloride-sensitive renal microangiopathy in the stroke-prone spontaneously hypertensive rat. *Kidney Int* 59: 1066-1076, 2001.

36. **Terker AS, Yang CL, McCormick JA, Meermeier NP, Rogers SL, Grossmann S, Trompf K, Delpire E, Loffing J, and Ellison DH**. Sympathetic stimulation of thiazide-sensitive sodium chloride cotransport in the generation of salt-sensitive hypertension. *Hypertension* 64: 178-184, 2014.

37. **Terker AS, Zhang C, McCormick JA, Lazelle RA, Zhang C, Meermeier NP, Siler DA, Park HJ, Fu Y, Cohen DM, Weinstein AM, Wang WH, Yang CL, and Ellison DH**. Potassium modulates electrolyte balance and blood pressure through effects on distal cell voltage and chloride. *Cell Metab* 21: 39-50, 2015.

38. **Ueno T, Nakashima A, Doi S, Kawamoto T, Honda K, Yokoyama Y, Doi T, Higashi Y, Yorioka N, Kato Y, Kohno N, and Masaki T**. Mesenchymal stem cells ameliorate experimental peritoneal fibrosis by suppressing inflammation and inhibiting TGF-beta1 signaling. *Kidney Int* 84: 297-307, 2013.

39. **Vallon V, Schroth J, Lang F, Kuhl D, and Uchida S**. Expression and phosphorylation of the Na+-Cl- cotransporter NCC in vivo is regulated by dietary salt, potassium, and SGK1. *Am J Physiol Renal Physiol* 297: F704-712, 2009.

40. **Velden J, Paust HJ, Hoxha E, Turner JE, Steinmetz OM, Wolf G, Jabs WJ, Ozcan F, Beige J, Heering PJ, Schroder S, Kneissler U, Disteldorf E, Mittrucker HW, Stahl RA, Helmchen U, and Panzer U**. Renal IL-17 expression in human ANCA-associated glomerulonephritis. *Am J Physiol Renal Physiol* 302: F1663-1673, 2012.

509 41. **Verlander JW, Hassell KA, Royaux IE, Glapion DM, Wang ME, Everett LA, Green**
510 **ED, and Wall SM**. Deoxycorticosterone upregulates PDS (Slc26a4) in mouse kidney: role of
511 pendrin in mineralocorticoid-induced hypertension. *Hypertension* 42: 356-362, 2003.
512 42. **Wesson DE**. Glomerular filtration effects of acute volume expansion: importance of
513 chloride. *Kidney Int* 32: 238-245, 1987.
514 43. **Wu J, Saleh MA, Kirabo A, Itani HA, Montaniel KR, Xiao L, Chen W, Mernaugh**
515 **RL, Cai H, Bernstein KE, Goronzy JJ, Weyand CM, Curci JA, Barbaro NR, Moreno H,**
516 **Davies SS, Roberts LJ, 2nd, Madhur MS, and Harrison DG**. Immune activation caused by
517 vascular oxidation promotes fibrosis and hypertension. *J Clin Invest* 126: 50-67, 2016.
518 44. **Xu J, Barone S, Brooks MB, and Soleimani M**. Double knockout of carbonic
519 anhydrase II (CAII) and Na(+)-Cl(-) cotransporter (NCC) causes salt wasting and volume
520 depletion. *Cell Physiol Biochem* 32: 173-183, 2013.
521 45. **Ziomber A, Machnik A, Dahlmann A, Dietsch P, Beck FX, Wagner H, Hilgers KF,**
522 **Luft FC, Eckardt KU, and Titze J**. Sodium-, potassium-, chloride-, and bicarbonate-related
523 effects on blood pressure and electrolyte homeostasis in deoxycorticosterone acetate-treated rats.
524 *Am J Physiol Renal Physiol* 295: F1752-1763, 2008.
525
526 **Figure captions**
527
528 **Fig. 1. Sodium chloride increased aldosterone-induced salt-sensitive hypertension and renal**
529 **dysfunction.**
530 (A) Line graph showing sequential blood pressure values measured once a week during the
531 observation period. (B) Graphs indicate urinary excretion of Na^+, Cl^-, K^+, and protein at week 0,

2, and 4 respectively. Na^+: sodium. Cl^-: chloride. K^+: potassium. Sham rats (sham): rats given water after left nephrectomy. Aldo/water rats (Aldo/water): hemi-nephrectomized rats drinking distilled water with aldosterone infusion. Aldo/$NaHCO_3$ rats (Aldo/$NaHCO_3$): hemi-nephrectomized rats drinking 1.44% $NaHCO_3$ with aldosterone infusion. Aldo/NaCl rats (Aldo/NaCl): hemi-nephrectomized rats drinking 1.0% NaCl with aldosterone infusion. Values are the mean ± SD. Blood pressure data and urinary data at each time point were analyzed using the general linear model, and statistical differences compared with Aldo/$NaHCO_3$ rats are indicated as § $P < 0.05$.

Fig. 2. Membranous expression of the Na^+-Cl^- transporter was enhanced in aldosterone and sodium chloride-treated rats.

(A) Representative immunoblot assay showing protein expression of transporters located at the aldosterone-sensitive distal nephron. (B) Quantification of protein expression of αENaC, pendrin, and total-NCC. (C) Representative immunoblot assay shows membrane expression of phosphorylated NCC, specifically T53, T58, and P71-NCC. (D) Quantification of protein expressions of phosphorylated NCC. αENaC: epithelial sodium channel alpha-subunit. NCC: thiazide-sensitive Na^+-Cl^- cotransporter. Sham rats (sham): rats given water after left nephrectomy. Aldo/water rats (Aldo/water): hemi-nephrectomized rats drinking distilled water with aldosterone infusion. Aldo/$NaHCO_3$ rats (Aldo/$NaHCO_3$): hemi-nephrectomized rats drinking 1.44% $NaHCO_3$ with aldosterone infusion. Aldo/NaCl rats (Aldo/NaCl): hemi-nephrectomized rats drinking 1.0% NaCl with aldosterone infusion. Values are the mean ± SD. Data were analyzed with ANOVA followed by Tukey's test. Statistical differences are indicated as * $P < 0.05$, ** $P < 0.01$.

555

556 **Fig. 3. Sodium chloride-treated rats showed increased aldosterone-induced renal injury.**

557 (A) Representative images of hematoxylin and eosin (H-E), Masson's trichrome (M-T), and

558 periodic acid-Schiff (PAS) staining showing typical morphological changes in renal tissue. (B)

559 Glomerulosclerosis scores. (C) Representative images of immunohistochemical staining showing

560 terminal deoxynucleotidyl transferase dUTP nick-end labeling (TUNEL)-positive cells, collagen

561 1, and alpha-smooth muscle actin (αSMA). (D) Quantification of TUNEL-positive cells, and

562 positive areas of collagen 1 and αSMA. (E) Representative immunoblot assay showing protein

563 expression levels of αSMA in sham rats, Aldo/water rats, Aldo/NaCl rats, and Aldo/$NaHCO_3$

564 rats. Glyceraldehyde-3-phosphate dehydrogenase (GAPDH) was used as an internal control.

565 Graph shows relative protein expression of αSMA. Sham rats (sham): rats given water after left

566 nephrectomy. Aldo/water rats (Aldo/water): hemi-nephrectomized rats drinking distilled water

567 with aldosterone infusion. Aldo/$NaHCO_3$ rats (Aldo/$NaHCO_3$): hemi-nephrectomized rats

568 drinking 1.44% $NaHCO_3$ with aldosterone infusion. Aldo/NaCl rats (Aldo/NaCl): hemi-

569 nephrectomized rats drinking 1.0% NaCl with aldosterone infusion. Values are the mean ± SD.

570 Parametric data were analyzed with ANOVA followed by Tukey's test. Glomerulosclerosis score

571 was analyzed with Kruskal-Wallis analysis followed by the Steel-Dwass test. Statistical

572 differences are indicated as * $P < 0.05$, ** $P < 0.01$.

573

574 **Fig. 4. Macrophages and T lymphocytes are associated with inflammation in aldosterone-**

575 **induced hypertensive rats.**

576 (A) Typical images of immunohistochemical staining for T lymphocytes (CD3-positive cells)

577 and macrophages (CD68-positive cells) showing inflammatory cell infiltration of kidneys of

sham rats, Aldo/water rats, Aldo/NaCl rats, and Aldo/$NaHCO_3$ rats. (B) Quantification of CD3- and CD68-positive cells. (C) Immunoblot assays showing protein expression of interleukin 17A (IL-17A). (D) Quantification of protein expression of IL-17A. Sham rats (sham): rats given water after left nephrectomy. Aldo/water rats (Aldo/water): hemi-nephrectomized rats drinking distilled water with aldosterone infusion. Aldo/$NaHCO_3$ rats (Aldo/$NaHCO_3$): hemin-ephrectomized rats drinking 1.44% $NaHCO_3$ with aldosterone infusion. Aldo/NaCl rats (Aldo/NaCl): hemi-nephrectomized rats drinking 1.0% NaCl with aldosterone infusion. Values are the mean ± SD. Data were analyzed with ANOVA followed with Tukey's test. Statistical differences are indicated as * $P < 0.05$, ** $P < 0.01$.

Fig. 5. Reduction of Cl^- intake prevented hypertension and inhibited protein expression of the Na^+-Cl^- transporter.

(A) Line graph indicates weekly dietary intake of control, high-Na/high-Cl, and high-Na/half-Cl groups during the observation period (n=8 for each group). (B) Line graph showing sequential blood pressure values measured biweekly. (C) Immunoblot assay showing membrane expression of αENaC, pendrin, total-NCC, T53, T58, and P71-NCC among control rats, high-Na/high-Cl rats, and high-Na/half-Cl rats. (D) Quantification of protein expression of αENaC, pendrin, total-NCC, T53, T58, and P71-NCC in the membrane fraction isolated from the kidney lysate. αENaC: epithelial sodium channel alpha-subunit. NCC: thiazide-sensitive Na^+-Cl^- cotransporter. Control rats (control): rats given a 0.26% NaCl (0.10% Na/0.16% Cl) diet. High-Na/high-Cl rats (high-Na/high-Cl): rats given an 8.0% NaCl (3.14% Na/4.85% Cl) diet. High-Na/half-Cl rats (high-Na/half-Cl): rats given a 4.0% NaCl 6.67% sodium citrate (3.14% Na/2.43% Cl) diet. All rats were subjected to hemi-nephrectomy and aldosterone infusion. Values are mean ± SD.

601 Dietary intake and blood pressure data at each time point were analyzed using the general linear
602 model, and statistical differences compared with high-Na/half-Cl rats are indicated as § $P < 0.05$.
603 Immunoblot data were analyzed with ANOVA followed by Tukey's test. Statistical differences
604 are indicated as * $P < 0.05$, ** $P < 0.01$.
605
606 **Fig. 6. Hydrochlorothiazide attenuated hypertensive nephropathy with inhibition of IL-17**
607 **and αSMA expression.**
608 (A) Line graph showing systolic blood pressure measured every week with or without
609 hydrochlorothiazide (HCTZ) treatment. (B) Changes in urinary protein per day. (C) Immunoblot
610 assay showing protein expression of alpha-smooth muscle actin (αSMA) and interleukin 17A
611 (IL-17A) in rats with and without HCTZ treatment. Glyceraldehyde-3-phosphate dehydrogenase
612 (GAPDH) was used as an internal control. (D) Quantification of protein expression of αSMA and
613 IL-17A. HCTZ-treated rats (HCTZ): Aldo/NaCl rats given 25 mg/kg/day hydrochlorothiazide by
614 oral gavage. Vehicle-treated rats (vehicle): Aldo/NaCl rats given distilled water. Values are the
615 mean ± SD. Blood pressure data at each time point were analyzed using the general linear model,
616 and statistical differences compared with vehicle-treated rats are indicated as § $P < 0.05$. The
617 other data were analyzed with Student's *t*-test for comparisons between two groups. Statistical
618 differences are indicated as * $P < 0.05$, ** $P < 0.01$.
619
620 **Fig. 7. Hydrochlorothiazide attenuated the protein expression level of Na^+-Cl^- transporter**
621 **and its phosphorylated forms in the membrane fraction.**
622 (A) Immunoblot assay showing membrane expression of Na^+-Cl^- transporters in Aldo/NaCl rats
623 with or without hydrochlorothiazide (HCTZ) treatment. (B) Quantification of protein expression

624 in the membrane fraction isolated from the kidney of Aldo/NaCl rats with or without HCTZ
625 treatment. HCTZ-treated rats (HCTZ): Aldo/NaCl rats given 25 mg/kg/day hydrochlorothiazide
626 by oral gavage. Vehicle-treated rats (vehicle): Aldo/NaCl rats given distilled water. Values are the
627 mean ± SD. Data were analyzed using Student's *t*-test for comparisons between two groups.
628 Statistical differences are indicated as * $P < 0.05$, ** $P < 0.01$.

Fig.1

A

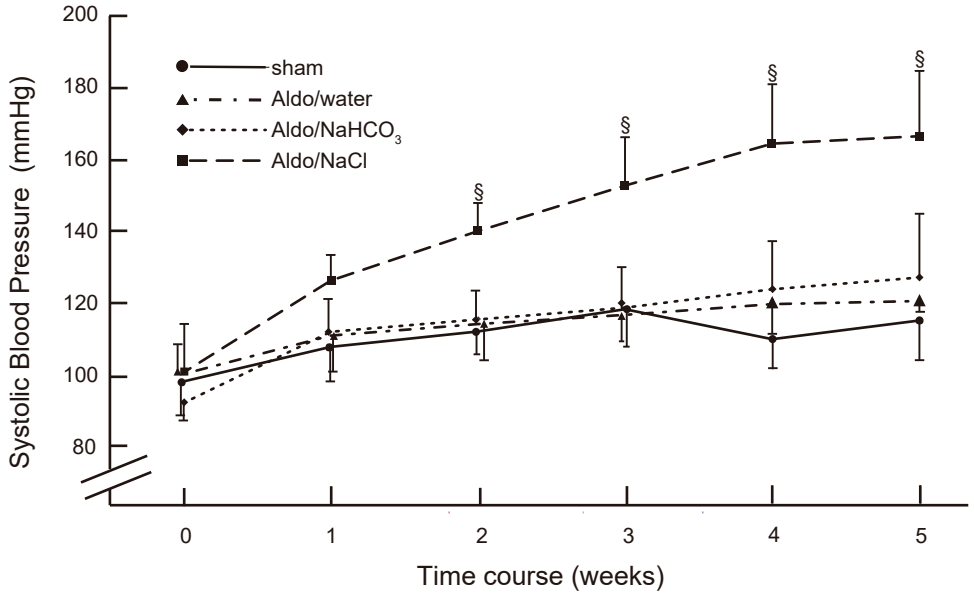
Systolic Blood Pressure (mmHg)
200
180
160
140
120
100
80
sham
Aldo/water
Aldo/NaHCO3
Aldo/NaCl
§
0
1
2
3
4
5
Time course (weeks)

B

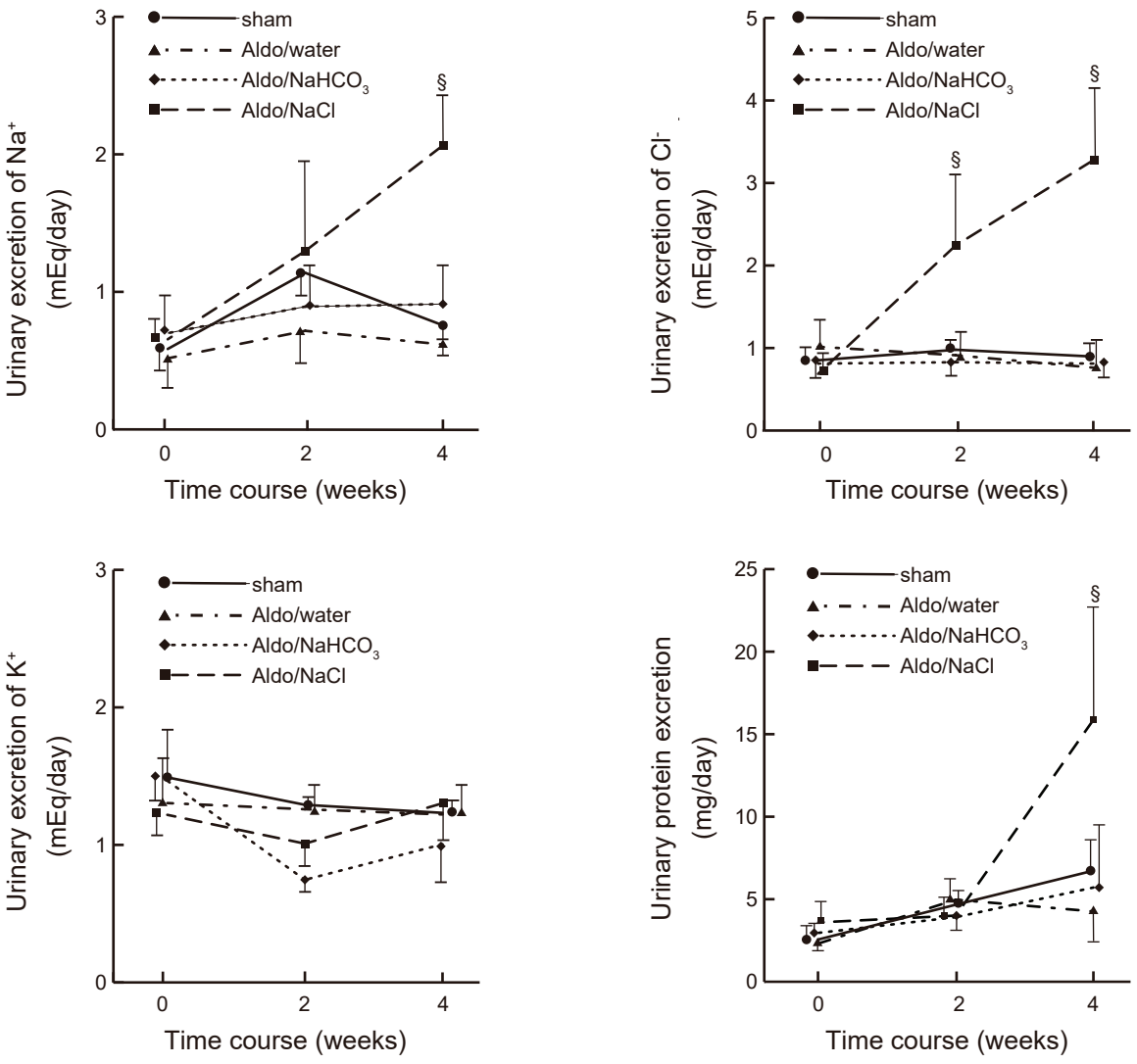
Urinary excretion of Na+ (mEq/day)
Urinary excretion of Cl- (mEq/day)
Urinary excretion of K+ (mEq/day)
Urinary protein excretion (mg/day)
sham
Aldo/water
Aldo/NaHCO3
Aldo/NaCl
§
Time course (weeks)

Fig.2

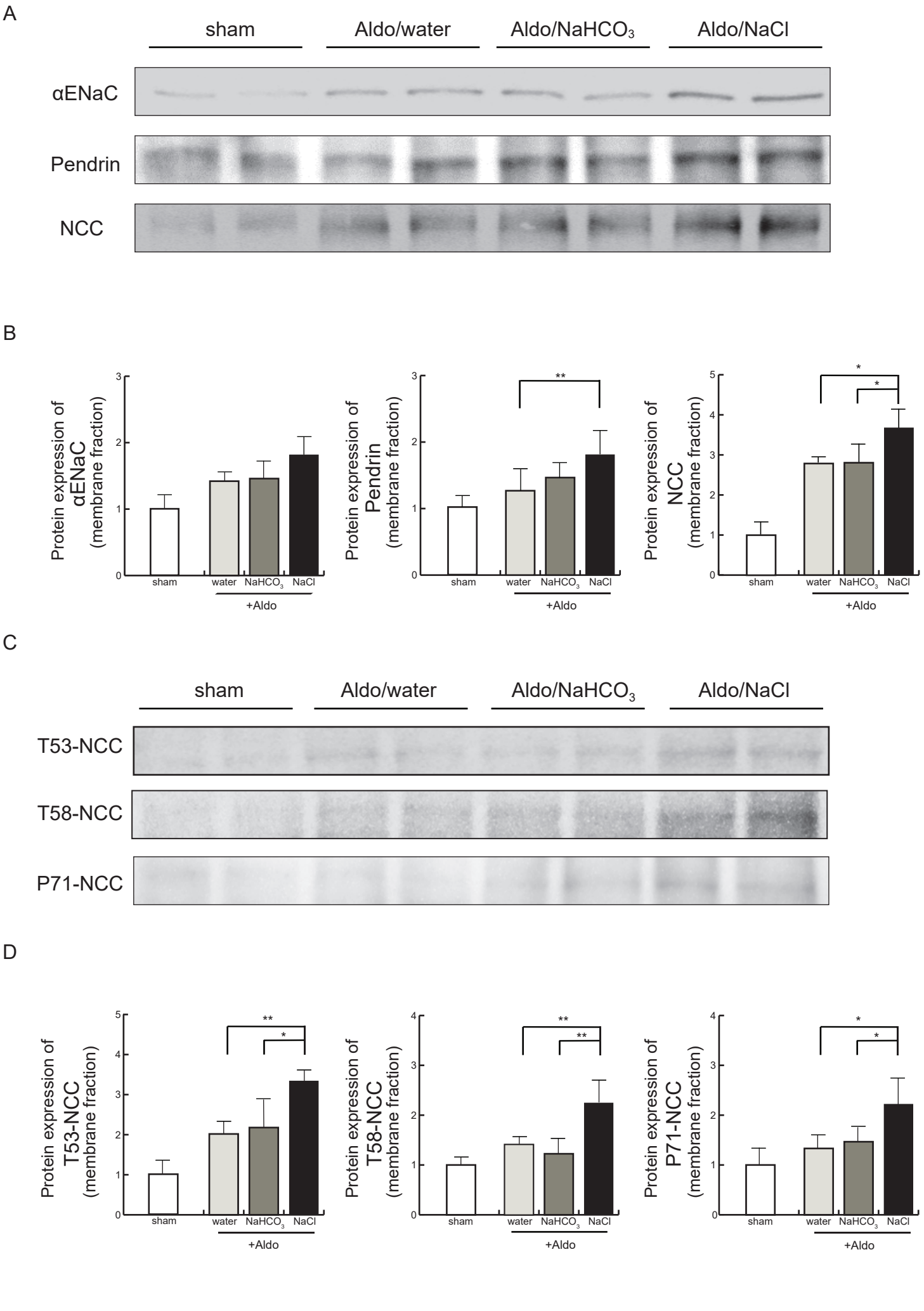
A
sham
Aldo/water
Aldo/NaHCO3
Aldo/NaCl
αENaC
Pendrin
NCC
B
Protein expression of αENaC (membrane fraction)
Protein expression of Pendrin (membrane fraction)
Protein expression of NCC (membrane fraction)
sham
water
NaHCO3
NaCl
+Aldo
C
sham
Aldo/water
Aldo/NaHCO3
Aldo/NaCl
T53-NCC
T58-NCC
P71-NCC
D
Protein expression of T53-NCC (membrane fraction)
Protein expression of T58-NCC (membrane fraction)
Protein expression of P71-NCC (membrane fraction)
sham
water
NaHCO3
NaCl
+Aldo

Fig.3

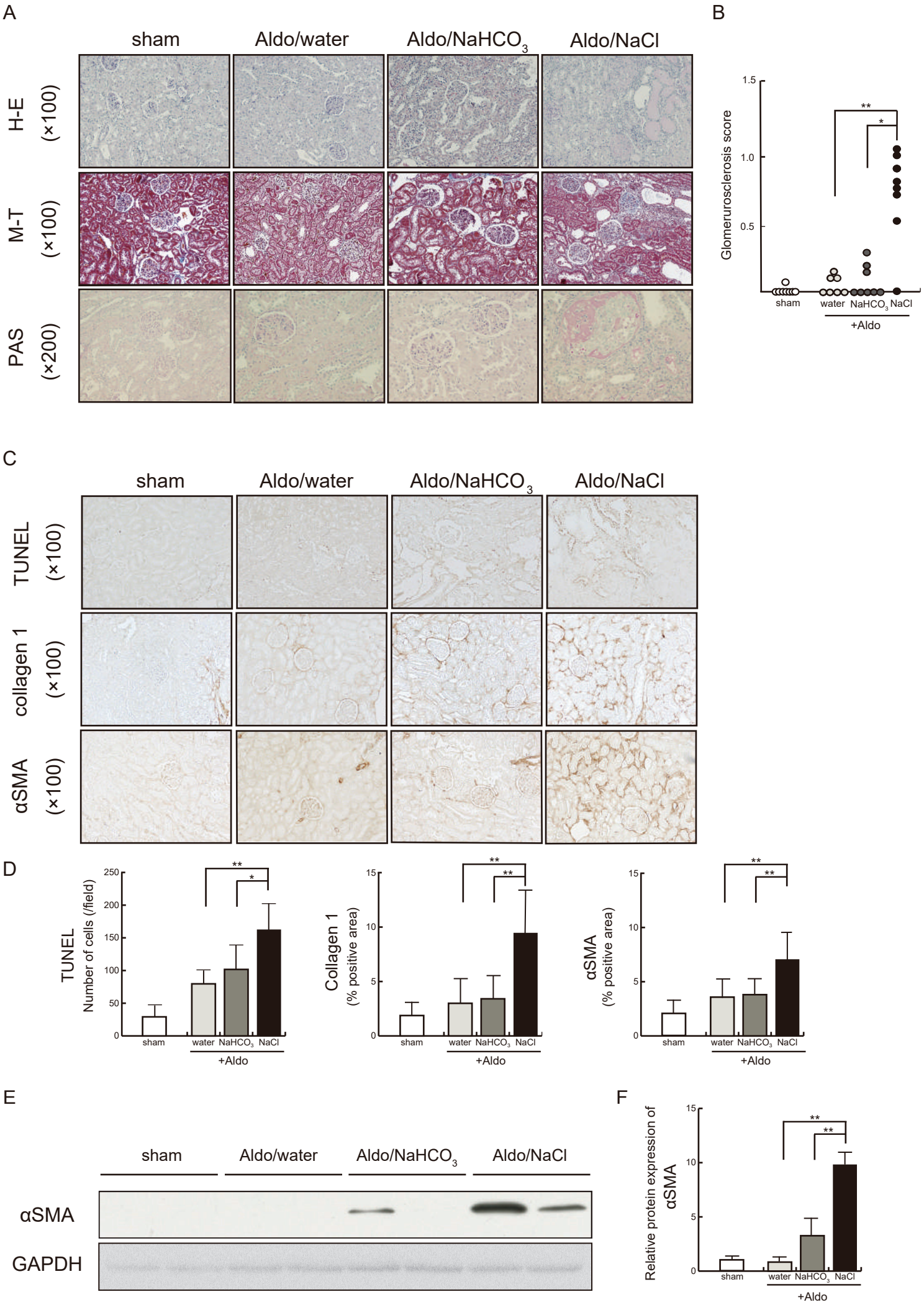
A
sham
Aldo/water
Aldo/NaHCO3
Aldo/NaCl
H-E (×100)
M-T (×100)
PAS (×200)
B
Glomerurosclerosis score
1.5
1.0
0.5
**
*
sham
water
NaHCO3
NaCl
+Aldo
C
sham
Aldo/water
Aldo/NaHCO3
Aldo/NaCl
TUNEL (×100)
collagen 1 (×100)
αSMA (×100)
D
TUNEL
Number of cells (/field)
250
200
150
100
50
0
Collagen 1
(% positive area)
15
10
5
0
αSMA
(% positive area)
sham
water
NaHCO3
NaCl
+Aldo
E
sham
Aldo/water
Aldo/NaHCO3
Aldo/NaCl
αSMA
GAPDH
F
Relative protein expression of αSMA
15
10
5
0
sham
water
NaHCO3
NaCl
+Aldo

Fig.4

A

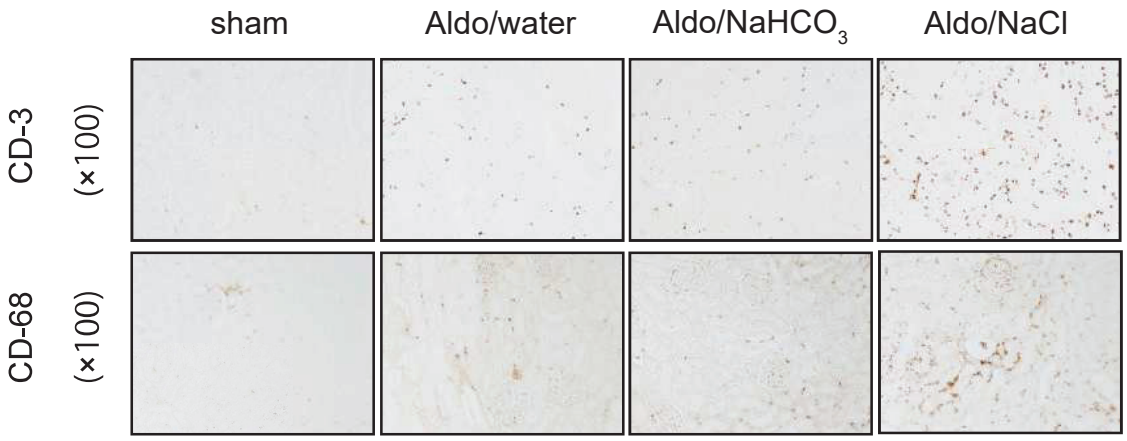
sham
Aldo/water
Aldo/NaHCO3
Aldo/NaCl
CD-3 (×100)
CD-68 (×100)

B

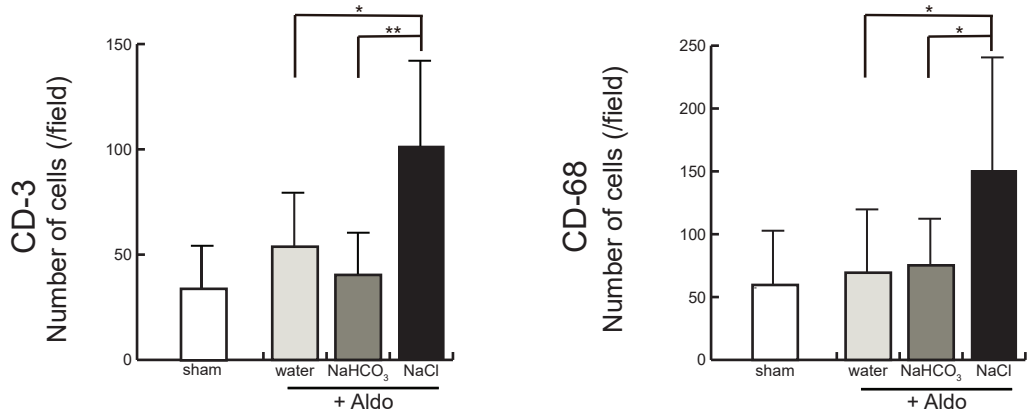
CD-3
Number of cells (/field)
150
100
50
0
*
**
sham
water
NaHCO3
NaCl
+ Aldo
CD-68
Number of cells (/field)
250
200
150
100
50
0
*
*
sham
water
NaHCO3
NaCl
+ Aldo

C

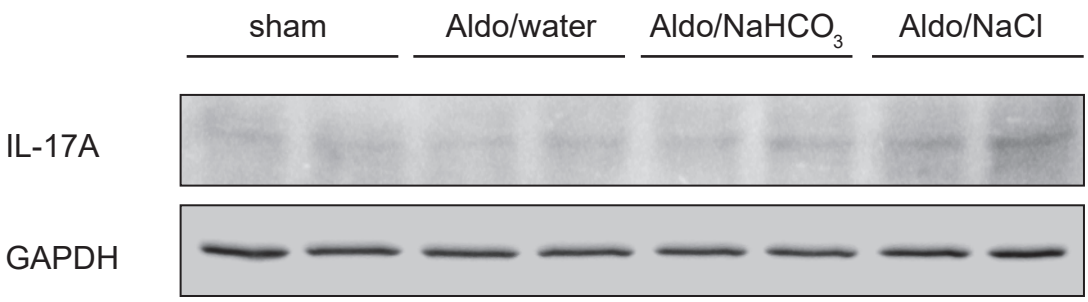
sham
Aldo/water
Aldo/NaHCO3
Aldo/NaCl
IL-17A
GAPDH

D

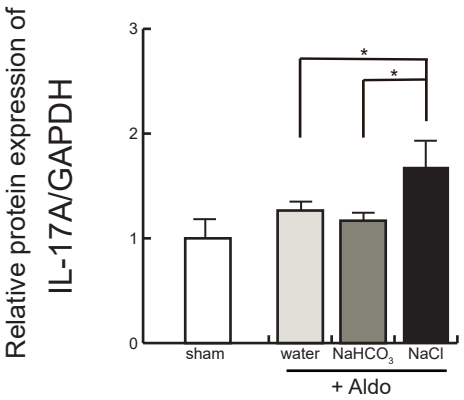
Relative protein expression of IL-17A/GAPDH
3
2
1
0
*
*
sham
water
NaHCO3
NaCl
+ Aldo

Fig.5

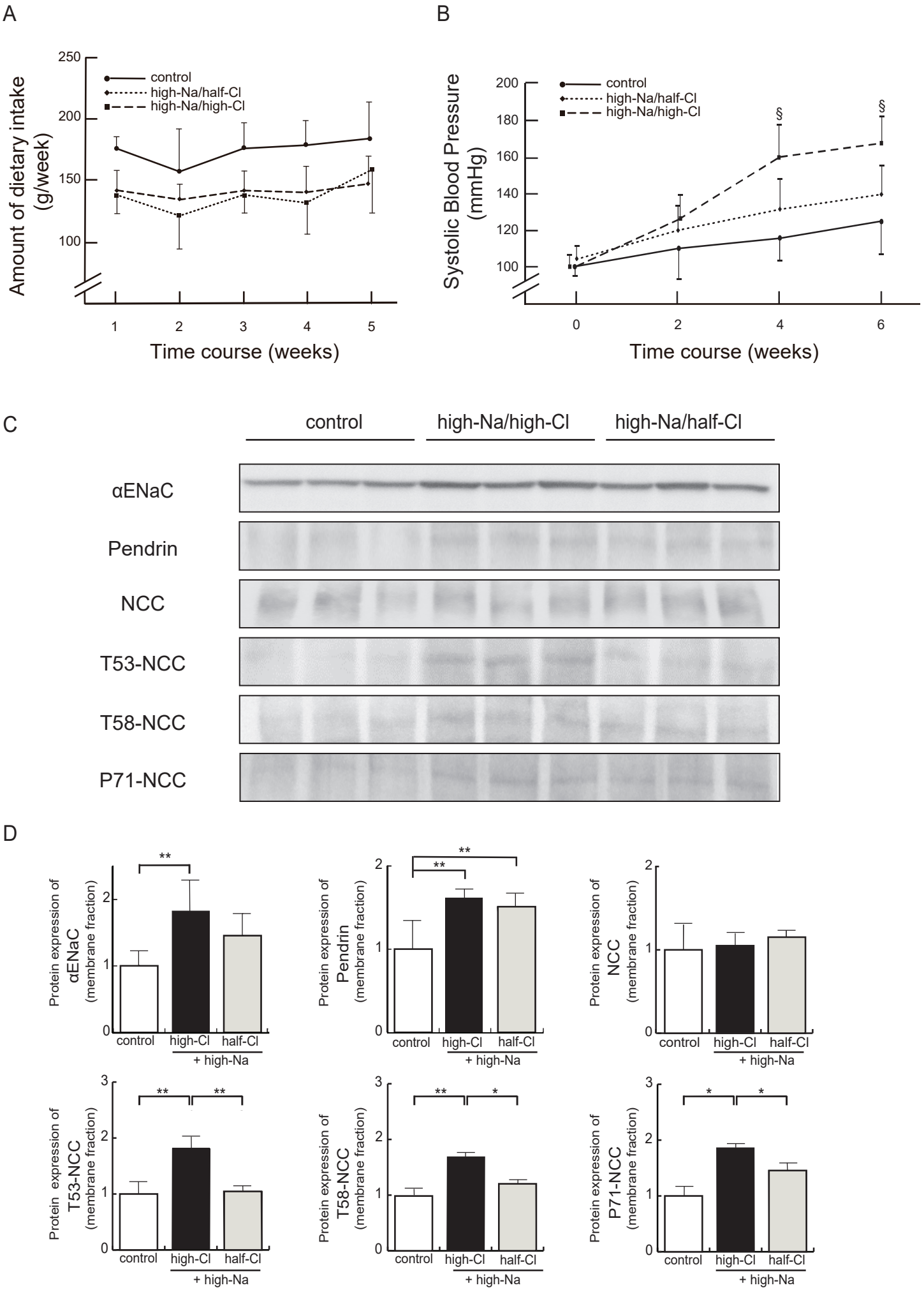
A
Amount of dietary intake (g/week)
250
200
150
100
control
high-Na/half-Cl
high-Na/high-Cl
1
2
3
4
5
Time course (weeks)
B
Systolic Blood Pressure (mmHg)
200
180
160
140
120
100
control
high-Na/half-Cl
high-Na/high-Cl
§
§
0
2
4
6
Time course (weeks)
C
control
high-Na/high-Cl
high-Na/half-Cl
αENaC
Pendrin
NCC
T53-NCC
T58-NCC
P71-NCC
D
Protein expression of αENaC (membrane fraction)
Protein expression of Pendrin (membrane fraction)
Protein expression of NCC (membrane fraction)
Protein expression of T53-NCC (membrane fraction)
Protein expression of T58-NCC (membrane fraction)
Protein expression of P71-NCC (membrane fraction)
control
high-Cl
half-Cl
+ high-Na
**
*

Fig.6

A

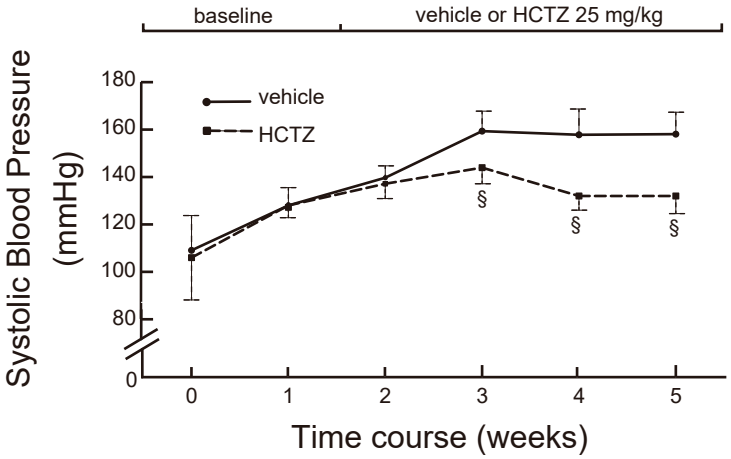
baseline
vehicle or HCTZ 25 mg/kg
Systolic Blood Pressure (mmHg)
vehicle
HCTZ
§
Time course (weeks)

B

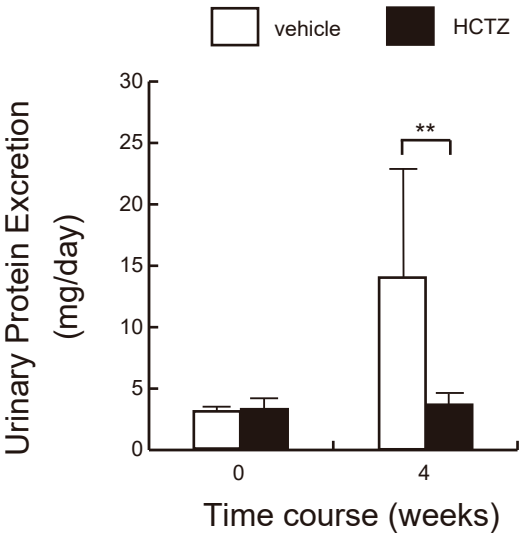
vehicle
HCTZ
Urinary Protein Excretion (mg/day)
**
Time course (weeks)

C

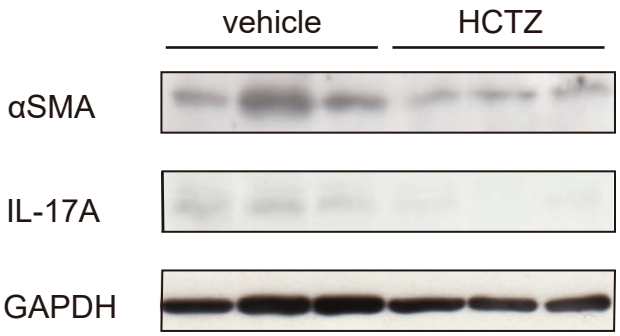
vehicle
HCTZ
αSMA
IL-17A
GAPDH

D

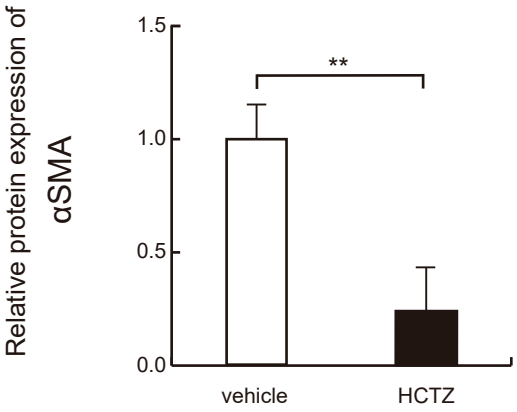
Relative protein expression of αSMA
**
vehicle
HCTZ

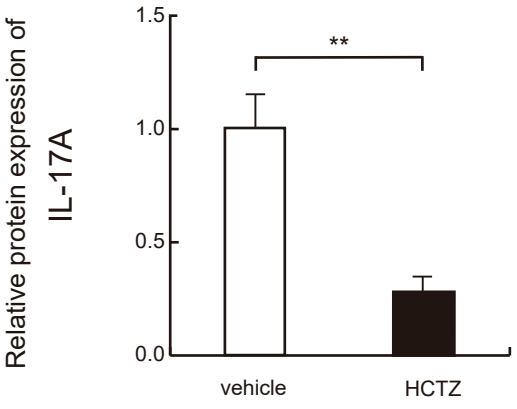
Relative protein expression of IL-17A
**
vehicle
HCTZ

Fig.7

A

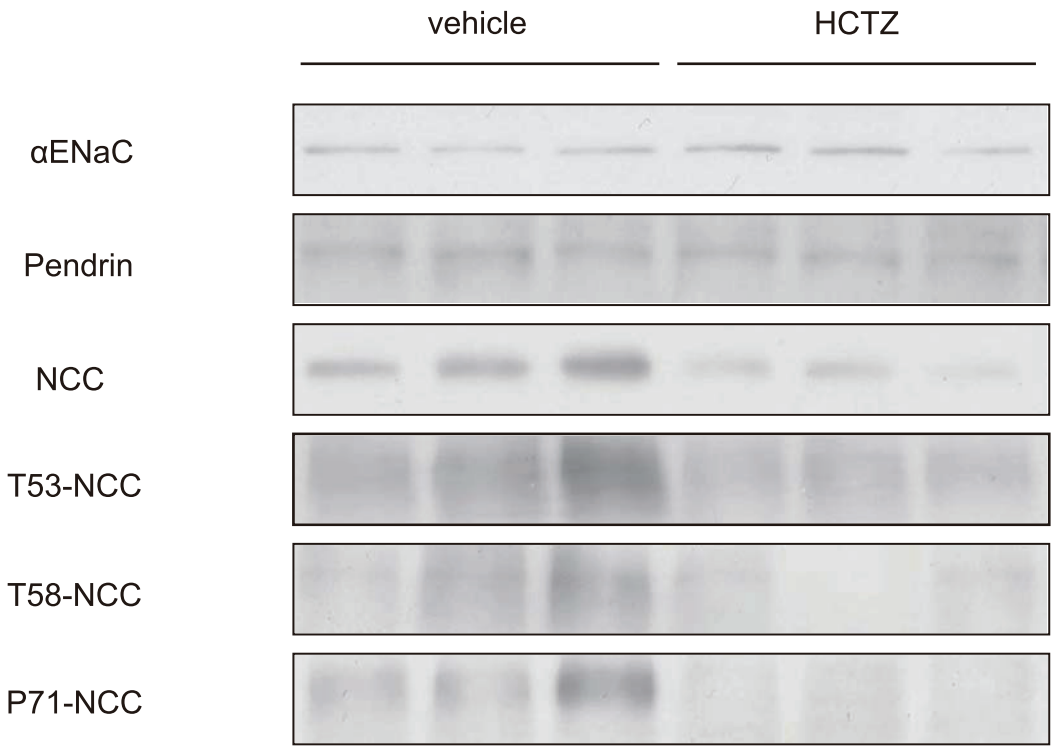
vehicle
HCTZ
αENaC
Pendrin
NCC
T53-NCC
T58-NCC
P71-NCC

B

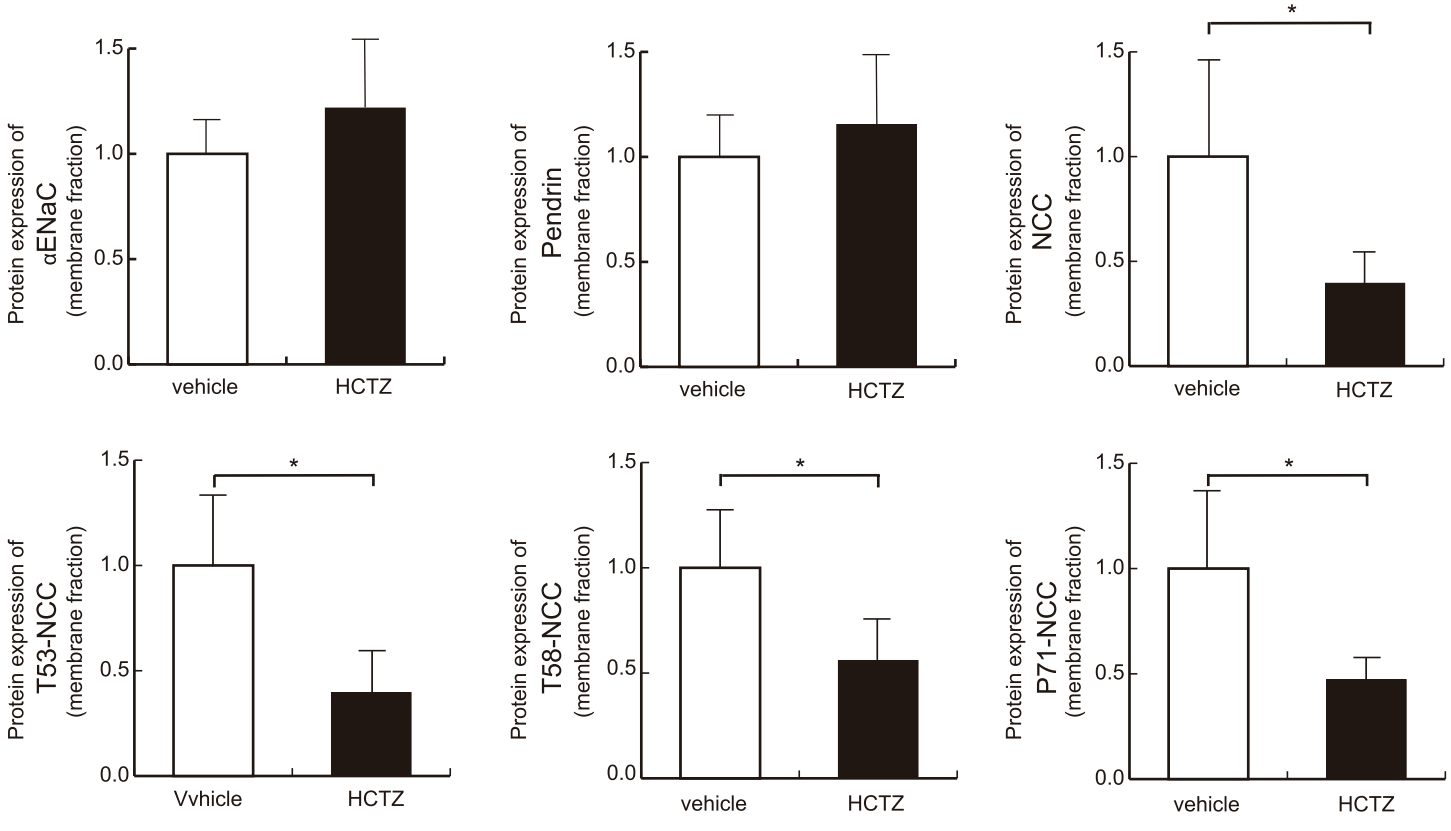
Protein expression of αENaC (membrane fraction)
Protein expression of Pendrin (membrane fraction)
Protein expression of NCC (membrane fraction)
Protein expression of T53-NCC (membrane fraction)
Protein expression of T58-NCC (membrane fraction)
Protein expression of P71-NCC (membrane fraction)
1.5
1.0
0.5
0.0
vehicle
HCTZ
Vvhicle
*